



# **Rollercoaster: An Efficient Group-Multicast Scheme for Mix Networks**

Daniel Hugenroth, Martin Kleppmann, and Alastair R. Beresford,  
*University of Cambridge*

<https://www.usenix.org/conference/usenixsecurity21/presentation/hugenroth>

**This paper is included in the Proceedings of the  
30th USENIX Security Symposium.**

**August 11-13, 2021**

978-1-939133-24-3

**Open access to the Proceedings of the  
30th USENIX Security Symposium  
is sponsored by USENIX.**

# Rollercoaster: An Efficient Group-Multicast Scheme for Mix Networks



Daniel Hugenroth  
*University of Cambridge*

Martin Kleppmann  
*University of Cambridge*

Alastair R. Beresford  
*University of Cambridge*

## Abstract

Mix network designs such as Loopix provide strong metadata anonymity guarantees that are crucial across many applications. However, because they limit the rate at which messages can be sent by each user, they incur high delays when sending many messages to multiple recipients – for instance, in decentralised collaborative apps.

In this paper we present an efficient multicast scheme named Rollercoaster that reduces the time for delivering a message to all members of a group of size  $m$  from  $\mathcal{O}(m)$  to  $\mathcal{O}(\log m)$ . Rollercoaster can be deployed without modifications to the underlying mix network, allowing it to benefit from the anonymity set provided by existing users. We further develop an extension that achieves the same asymptotic guarantees in the presence of unreliable group members.

While the scheme is applicable to many mix network designs, we evaluate it for the Loopix network, which is the most advanced and practical design to date. For this evaluation we developed a network simulator that allows fast, reproducible, and inspectable runs while eliminating external influences.

## 1 Introduction

Information security often focuses on the confidentiality and integrity of electronic messages. However, metadata privacy is frequently also important since merely knowing the parties involved in a communication can reveal sensitive information and stigmatise groups and individuals. For example, revealing the names of people contacting a sexual health clinic may discourage individuals from seeking treatment; and potential whistle-blowers may be dissuaded from disclosing illegal or unethical behaviour to a journalist. Strong metadata privacy is critical across many domains, not just healthcare and journalism, but also in diplomatic services and military operations.

Protecting metadata privacy is not merely a theoretical requirement: we find ourselves in an era of mass-surveillance by well-funded state actors as well as pervasive data collection by private companies and service providers. In this reality

there are many online applications where protecting metadata privacy is of practical importance.

The Tor [1] network is perhaps the best known example of a system that provides metadata privacy. Tor brought so-called anonymous communication networks to a large audience by providing low-latency communication and anonymous access to the Internet. However, while the Tor network provides high throughput and low latency, it does not provide metadata privacy in the presence of a global adversary who can observe all communication [2]. Mix network designs and broadcast schemes provide metadata privacy in the face of global adversaries, however they do so at the cost of significantly higher latency and lower overall throughput. A prominent recent medium-latency mix network design, which protects metadata privacy in the presence of a global adversary, is Loopix [3].

Many *collaborative apps* are in use today, including group messaging services such as WhatsApp, Signal, and iMessage; productivity tools such as Google Docs and Office365; and file sharing applications such as Dropbox and Box. At present, no mainstream collaborative apps provide metadata privacy. Hence, in this paper, we present a new architecture that enables strong metadata privacy for such applications.

We consider forms of collaboration in which a file or conversation thread is shared by a group of collaborators, and any update to it needs to be shared with all group members. Group messaging and collaboration can share the same underlying infrastructure [4]. In collaborative editing applications individual update messages are usually small and frequent [5]. Such apps therefore require an efficient, reliable, and timely method of sending messages to all members of a group. However, the original design of Loopix provides only one-to-one (unicast) messages, and no built-in mechanism for group communication (multicast). In this paper we show that naïvely implementing multicast in an anonymity network like Loopix results in significant overhead in terms of latency and throughput, typically exceeding the latency required to provide good user experience. We therefore extend Loopix to support low-latency group communication while preserving metadata privacy.

This paper makes the following contributions:

- An anonymous group communication scheme called *Rollercoaster*, which achieves a group multicast latency of  $\mathcal{O}(\log m)$  for groups of size  $m$ , while ensuring strong metadata privacy against an active global adversary (§5). In our evaluation Rollercoaster achieves a 99th percentile ( $p_{99}$ ) latency of 12.3 seconds for groups larger than 100 users, whereas the default implementation of Loopix incurs a latency of 75.6s (§6.2). Rollercoaster works by involving many group members, not just the sender of a message, in the task of disseminating a message.
- An extension to the Rollercoaster scheme that adds fault-tolerance to gracefully handle the fact that some group members may be offline, while preserving scalability (§5.2). Even in the presence of faulty nodes, Rollercoaster performs better than default Loopix for mean,  $p_{90}$ , and  $p_{99}$  latency. Our solution reduces  $p_{99}$  latency to 21.9s compared to 103.3s for default Loopix (§6.3) when evaluated against realistic connectivity patterns.
- The design of the *MultiSphinx* packet format that allows limited multicast by designated mix nodes while preserving strong metadata privacy guarantees (§5.4).
- A deterministic, open-source simulator for Loopix and Rollercoaster that allows efficient, inspectable, and reproducible performance evaluations. We use it to empirically compare the latency properties of both systems. Compared to evaluations using a real network, it reduces the required CPU hours by a factor of 4500 $\times$ , allowing us to explore significantly more scenarios and parameter choices (§6.1).

## 2 Threat Model and Goals

Our work guarantees strong anonymity against sophisticated adversaries while providing an efficient, low-latency, and fault-tolerant group-multicast anonymity network.

**Assumptions** We assume three types of participants in a mix network based on the Loopix model [3]: *Users* are members of one or more groups; group members can broadcast and receive messages to and from all members of the group. *Provider nodes* act as the users' entry points to the anonymity network; all communication to or from a specific user flows through their provider. *Mix operators* manage a mix node in the core of the network; mix nodes receive messages from other mix nodes or providers and send messages to other mix nodes or providers. Mix nodes do not communicate directly with users. For further details on the Loopix model and how these participants communicate, see Section 3.

**Security and Anonymity** We assume a global active adversary who can observe all traffic, manipulate traffic to remove messages and insert new ones, as well as corrupt a subset of mix nodes and providers. As in Loopix, sending a message to a Rollercoaster user requires that the sender knows both the addresses and public keys for their provider, the recipient, the recipient's provider, and the mix nodes.

Our scheme provides message confidentiality and integrity as well as the same strong metadata privacy guarantees as Loopix, including *sender-recipient unlinkability* (preventing an adversary from deducing which users are communicating with each other) and *sender/recipient online unobservability* (preventing an adversary from deducing which users are currently participating in any communication). More details on these and further definitions of metadata privacy are given by Pfitzmann and Hansen [6]. In addition we provide *membership unobservability* (preventing anyone outside the group from determining group membership or group size). We assume a group is composed of trusted members and therefore we do not provide unlinkability or unobservability guarantees against an attacker who compromises or colludes with group members. The goal of the attacker is to break the confidentiality, integrity, or metadata privacy guarantees.

Our scheme supports efficient communication for group sizes of two or more and therefore we handle pairwise and group communication in the same way. An attacker cannot distinguish between two-party communication and communication in a larger group.

**Application Requirements** Low latency is often a requirement in group communication. For example, user studies have highlighted the negative implications of high network delays in collaborative editing. One previous study [7] asked a group of participants to transcribe audio lectures using collaborative text editing software. The researchers investigated the effect of communication latency by repeating the experiment multiple times and varying artificial delay on all communication between participants. A delay of 10 seconds or more had a significant impact in their study, with an increase of error rates and content redundancy by more than 50%. We therefore set our target for group multicast latency at 10 seconds for group sizes of up to 100 people. The group size is motivated by the active editor limit of Google Docs (100 users) and Microsoft Sharepoint (99 users). We further require the latency to grow sub-linearly with the size of the group, allowing effective collaboration in large groups. In many multi-user applications, a large fraction of the data is generated by a small fraction of the users (a trend that is known as *participation inequality* [8]), and our scheme fares well in a system with such a distribution of activity.

Offline support is required since mobile devices do not always have connectivity. As in the Loopix design, provider nodes in Rollercoaster store messages on behalf of the user until the user is next online and able to download them.

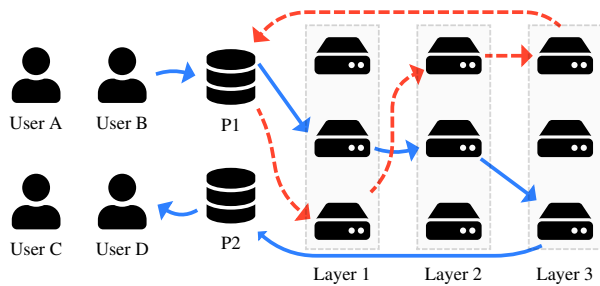


Figure 1: Schematic for a Loopix network with four users (A, B, C, D), two providers (P1, P2), and a three-layer mix network. Each node of mix layer  $L$  is connected to each node of layer  $L + 1$ . The solid blue arrows depict one possible path for a payload or drop message from user  $B$  to user  $D$ . The dashed red line represents loop traffic induced by a mix node.

On mobile devices, the frequency of sending network packets has a large impact on energy efficiency. Every transmission promotes the mobile network connection from idle to an active sending state after which it remains in a tail state for a few seconds [9, §5.1]. During the active sending/receiving state (1680 mW, data for LTE) and the tail state (1060 mW) the power consumption is higher than during idle (594 mW) [9, Table 3]. Every promotion from idle to active comes with additional energy costs. Therefore, sending few but large messages with long intra-packet pauses is advantageous for battery life on mobile devices, even if the total volume of data transmitted is the same. On the other hand, smaller and more frequent messages lead to lower latency.

We assume that the group membership is fixed and known to all members; we leave the problems of group formation and adding or removing group members for future work.

### 3 Background

Our work builds on Loopix, which we introduce in this section. Section 3.2 introduces multicast as it is used in this paper.

#### 3.1 Loopix

Loopix is a mix network [10]: messages are sent via several mix nodes to conceal their sender and destination. The route is chosen by the sender and encoded in message headers.

Several mix network designs have been proposed: for example, in the *threshold* approach, a mix node waits until a fixed number of messages have arrived, and then forwards them to their next hops in a random order. A mix node must wait for a sufficient number of messages to arrive before forwarding them to ensure there is significant uncertainty in the mapping between incoming and outgoing messages. Unfortunately, this batching process can lead to high latency.

Loopix takes a different approach to mixing: whenever a

message passes through a node, it delays that message by a duration  $d_\mu$ . For each hop the sender independently chooses  $d_\mu$  randomly from the exponential distribution with rate parameter  $\lambda_\mu$ , and includes that value in the message header.

Moreover, Loopix ensures that the timings of messages sent by any node can be modelled as a *Poisson process* (i.e. the interval between messages is exponentially distributed). Applying exponentially distributed random delay to a Poisson process yields another Poisson process; moreover, aggregating the events from several Poisson processes yields another Poisson process [3]. Message senders can adjust  $\lambda_\mu$  to balance the trade-off between reducing latency (increase  $\lambda_\mu$ ) and strengthening anonymity (decrease  $\lambda_\mu$ ).

An individual mix node may be compromised by the adversary, allowing it to learn the mapping between input and output messages. However, a mix network provides strong anonymity guarantees when at least one of the mix nodes on the message’s path is trustworthy. Cover traffic is added to hide communication patterns and to prevent an attacker from inferring message senders and recipients merely by looking at the set of messages sent and received over time.

Loopix arranges mix nodes in  $l$  layers (where  $l = 3$  is a typical choice), forming a *stratified topology*. In this arrangement, each node is connected to all nodes of the next layer, and a message flows through one mix node in each layer. The system’s message throughput capacity can be increased by adding more nodes to each layer.

Access to the mix network is mediated by provider nodes (see Figure 1). Providers receive and store incoming messages for each user in an inbox, allowing the end-user device to be offline and download messages from the provider later. These messages are still end-to-end encrypted and providers cannot distinguish them from cover traffic (see below). The provider nodes are a required component if the end-user device (e.g. smartphone) is not always connected to the Internet. Moreover, the provider nodes support revenue generation since the provider can charge users to cover operating costs without knowing who their customers are communicating with.

##### 3.1.1 Messages and Traffic

All Loopix messages are encrypted and padded to a fixed size<sup>1</sup> using the Sphinx [11] mix message format. The Sphinx message format uses layered encryption and ensures the contents of messages change at every hop in the mix network. Fixed-size padding renders messages containing payload traffic indistinguishable from cover traffic messages. This approach means the attacker cannot correlate incoming and outgoing messages based on payload contents or length. Loopix uses three types of messages:

**Drop messages** are the primary form of cover traffic. They are sent by users as a Poisson process with rate parameter  $\lambda_d$

<sup>1</sup>The implementation accompanying the original Loopix paper uses a message size of 1024 bytes, including headers and overheads.

$d_p \sim \exp(\lambda_p)$	Delay between successive payload messages
$d_d \sim \exp(\lambda_d)$	Delay between successive drop messages
$d_l \sim \exp(\lambda_l)$	Delay between successive loop messages
$d_\mu \sim \exp(\lambda_\mu)$	Delay applied on message forwarding
$\Delta_{pull}$ (constant)	Polling interval for checking inboxes
$d_M \sim \exp(\lambda_M)$	Delay between successive loop messages sent by mix nodes

Table 1: Delays are either constant or chosen from an exponential (exp) distribution with the given parameter. Our notation slightly differs from the original paper.

and addressed to a randomly chosen user’s inbox. They follow the full transport route from the sender’s provider through all layers of the mix network to the recipient’s device. Recipients download the message from their inboxes, decrypt it, and only then identify it as drop traffic and discard it.

**Payload messages** contain application data and are sent as a Poisson process with rate parameter  $\lambda_p$ . When an user sends multiple messages in quick succession, they are added to a send queue at the client and forwarded to the user’s provider at an average rate of  $\lambda_p$ . While they are in the payload send queue, messages experience delay  $d_Q$ . When there are no payload messages waiting to be sent, a drop message is sent instead. Keeping the send rate constant prevents irregular traffic patterns that may reveal whether a user is currently actively communicating.

**Loop messages** defend against active attacks such as  $(n - 1)$  attacks [12]. In such an attack an adversary tries to follow the path of a message by blocking all other incoming traffic for the mix node or replacing it with its own. Loop messages are injected by both users (at rate  $\lambda_l$ ) and mix nodes (at rate  $\lambda_M$ ); these messages travel in a loop though all mix layers, via a provider node, back to the sender. If the loop messages sent by a node fail to be delivered back to that node, it can suspect that an active attack is taking place and employ countermeasures as described in the Loopix paper [3, §4.2.1].

Choosing suitable rate parameters depends heavily on the application behaviour, the message size, and the capacity of the underlying network. In the original Loopix paper the values of the parameters  $\lambda_p$ ,  $\lambda_d$ , and  $\lambda_l$  range from one message per second to one message per minute. With a total message size of  $|msg|$  bytes and the rates given in messages/s, the required bandwidth of a client can be estimated as  $(\lambda_p + \lambda_d + \lambda_l) \cdot |msg|$  bytes/s.

### 3.2 Multicast and Group Messaging

A *multicast* protocol allows a single message to be delivered to all members of a group. Broadly speaking, there are two

approaches for implementing multicast: by sending each message individually to each recipient over unicast, or by relying on the underlying network to make copies of a message that are delivered to multiple recipients. IP multicast [13] is an example of the latter approach, which avoids having to send the same message multiple times over the same link.

In this paper we are interested in *group multicast*, a type of multicast protocol in which there is a pre-defined, non-hierarchical group of users  $U$ . At any time any member of the group might send a message to all other group members. We call the initial sender *source*  $s$  and all others the intended recipients  $U_{recv} = U \setminus s$ .

## 4 Naïve Approaches to Multicast

In this section we discuss the reasons why message delays occur in Loopix. We then explore two simple approaches to implementing multicast on Loopix, and explain why they are not suitable, before introducing Rollercoaster in Section 5.

We define the message latency  $d_{msg}$  of a single unicast message  $msg$  from user to  $A$  to user  $B$ :

$$d_{msg} = T_{recv,B} - T_{send,A} \quad (1)$$

where  $T_{send,A}$  is the time at which user  $A$ ’s application sends  $msg$ , and  $T_{recv,B}$  is the time at which user  $B$ ’s application receives the message.

In Loopix, message delays are the sum of delays at various points in the network. First, any outbound message sent by the user to the provider experiences a queuing delay  $d_Q$  based on the number of messages in the send queue. The delay between two successive messages in the queue being sent,  $d_p$ , is exponentially distributed with a rate parameter  $\lambda_p$  (see Table 1). Hence, a message’s time spent in the send queue,  $d_Q$ , is a random variable with a Gamma distribution  $\Gamma(n, \frac{1}{\lambda_p})$ , where the shape parameter  $n$  denotes the number of messages in the queue ahead of our message  $msg$ .

Secondly, the payload message is held up at the ingress provider and each of the  $l$  mix nodes by an exponentially-distributed delay  $d_\mu$ . Finally, the receiving user checks their inbox in fixed time intervals of  $\Delta_{pull}$ , leading to a delay  $d_{pull}$  that is uniformly distributed between 0 and  $\Delta_{pull}$ . Therefore the message delay in a Loopix network with  $l$  layers can be expressed as a sum of these components:

$$d_{msg} = d_Q + d_p + (l + 1) \cdot d_\mu + d_{pull} \quad (2)$$

The above equation ignores processing and network delays. The Loopix paper demonstrates that these are negligible compared to the delays imposed by sensible rate parameters.

For a Poisson distribution with parameter  $\lambda$ , the expected mean is  $1/\lambda$ . The Gamma distribution  $\Gamma(n, \frac{1}{\lambda_p})$  has the mean  $\frac{n}{\lambda_p}$ . For the pull interval, the expected mean delay is  $\Delta_{pull}/2$ .

Hence, the mean latency for Equation 2 is:

$$\text{mean}(d_{msg}) = \frac{n+1}{\lambda_p} + \frac{l+1}{\lambda_\mu} + \frac{\Delta_{pull}}{2} \quad (3)$$

When a source  $s$  wants to send a payload to a group by multicast, we define the *multicast latency*  $D$  to be the time from the initial message sending until all of the recipients  $U_{recv}$  have received the message:

$$D = \max_{u \in U_{recv}} (T_{recv,u}) - T_{send,s} \quad (4)$$

## 4.1 Naïve Sequential Unicast

In the simplest implementation of multicast, the source user  $s$  sends an individual unicast message to each of the recipients  $u \in U_{recv}$  in turn. While the messages can travel through the mix network in parallel, their emission rate is bounded by the payload rate  $\lambda_p$  of the sender.

For a recipient group of size  $|U_{recv}| = m - 1$ , the last message in the send queue will be behind  $n = m - 2$  other messages. Further, the last message will incur the same network delay and pull delay as all other unicast messages. The average delay for the last message therefore describes the multicast latency for when performing sequential unicast:

$$D_{unicast} = \frac{m-1}{\lambda_p} + \frac{l+1}{\lambda_\mu} + \frac{\Delta_{pull}}{2} = \mathcal{O}(m) \quad (5)$$

The mean delay  $D_{unicast}$  therefore grows linearly with  $m$ . As we show in Section 6, sequential unicast is too slow for large groups with realistic choices of parameters ( $\lambda_p$  is typically set to less than one message per second).

Another problem with the sequential unicast approach is that the effective rate at which a user can send messages to the group is  $\frac{\lambda_p}{m-1}$ , as all copies of the first message need to be sent before the second multicast message can begin transmission.

One might argue that this problem can be addressed by increasing the payload bandwidth by increasing the value for  $\lambda_p$ . However, this would require similar adjustments to the rates for drop and loop messages to preserve the network's anonymity properties. As these parameters are fixed across all users, this would lead to a proportional increase in overall bandwidth used by the network. Moreover, the factor by which we increase  $\lambda_p$  would be determined by the largest group size we want to support. As a result, users participating in smaller groups would face an unreasonable overhead. This inefficiency particularly applies to users who mostly receive and only rarely send messages.

## 4.2 Naïve Mix-Multicast

An alternative approach shifts the multicast distribution of a message to mix nodes. In this scheme, the source chooses one mix node as the *multiplication node*. This node receives

a single message from the source and creates  $|U_{recv}| = m - 1$  mix messages sent on to the other group members. A provider node would not be suitable as a multiplication node as it would learn about the group memberships of its users and their group sizes.

When the multiplication node receives such a multicast message, it inserts  $m - 1$  messages into its input buffer, one for each of the recipients, and processes them as usual. This provides optimal group message latency of  $D = d_{msg}$  as there is no rate limit on messages sent by a mix node, and hence no queuing delay. However, this design has significant flaws.

First, a corrupt multiplication mix node can learn the exact group size  $|U| = m$ , in contravention of our threat model. This is undesirable as it may allow an attacker to make plausible claims regarding the presence or absence of communication within certain groups. Even without corrupting a node, an adversary can observe the imbalance between incoming and outgoing messages of a multiplication node.

The weakened anonymity properties could perhaps be mitigated with additional cover traffic that incorporates the same behaviour as the payload traffic. In particular, the cover traffic must model all possible group sizes. Allowing a group size of 200 requires cover traffic to multicast by factor 200 as well. However, this would significantly increase the network bandwidth requirements in the following mix layers, increasing the cost of operating the network.

Permitting message multiplication also opens up the risk of denial of service attacks: a malicious user could use the multicast feature to send large volumes of messages to an individual provider, mix node, or user, while requiring comparatively little bandwidth themselves.

Finally, supporting group multicast in a mix node requires the input message to contain  $m - 1$  payloads and headers, one for each outgoing message. As all outgoing messages must travel independently of each others they must be encrypted with different keys for their respective next hops. Otherwise, all outgoing messages share the same encrypted payload. This makes it trivial for an observer to identify the recipients of this group message. The only solution is to either increase the size of *all* messages in the system or enforce a very low limit on maximum group size.

In summary, naïvely performing message multiplication on mix nodes is not a viable option. However, a viable variant of this approach is possible by fixing the multiplication factor of messages to be a small constant (e.g.  $p = 2$ ). We discuss this design in Section 5.4 where we present MultiSphinx.

## 5 Rollercoaster

We propose *Rollercoaster* as an efficient scheme for group multicast in Loopix. Rollercoaster distributes the multicast traffic over multiple nodes, arranged in a distribution graph. This not only spreads the message transmission load more uniformly across the network, but it also improves the balance

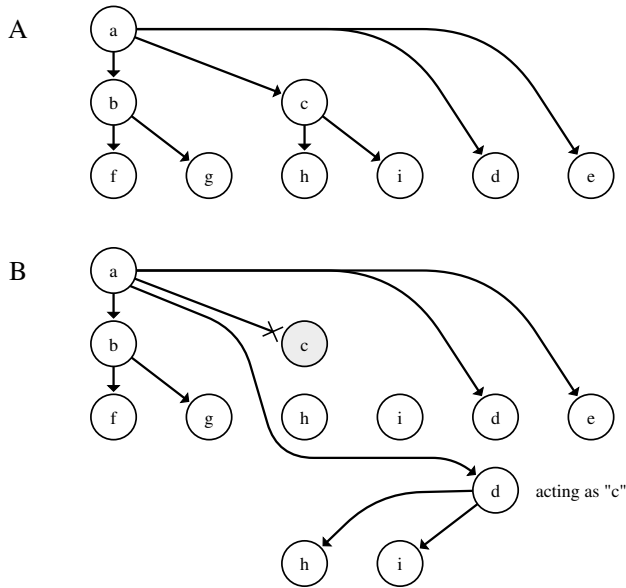


Figure 2: Message distribution graph for a group of size  $m = 8$  and branching factor  $k = 2$ . *Graph A*: Expected delivery from source  $s = a$ . *Graph B*: The node  $c$  is offline and breaks delivery to  $h$  and  $i$ . Using the fault-tolerant variant the node  $d$  is assigned the role of  $c$  and delivers the payload to  $h$  and  $i$ .

of payload and cover traffic. Rollercoaster is implemented as a layer on top of Loopix, and it does not require any modifications to the underlying Loopix protocol (we discuss an optional protocol modification in Section 5.4).

As we have seen with naïve sequential unicast, messages slowly trickle from the source into the network as the source’s message sending is limited by the payload rate  $\lambda_p$ . However, users who have already received the message can help distribute it: after the source has sent the message to the first recipient, both of them can send it to the third and fourth recipient concurrently. Subsequently, these four nodes then can send the message to the next four recipients, and so on, forming a distribution tree with the initial source at the root.

The distribution tree for a set of users  $U$  is structured in *levels* such that each parent node has  $k$  children at each level, until all recipients have been included in the tree. An example with eight recipients is shown in Figure 2. With each level the total number of users who have the message increases by a factor of  $k + 1$ , which implies that the total number of levels is logarithmic in the group size  $|U|$ .

In this section we first detail the construction of Rollercoaster in Section 5.1. As a second step, Section 5.2 adds fault tolerance to ensure that the scheme also works when nodes are offline. Asymptotic delay and traffic properties are analysed in Section 5.3. Section 5.4 develops the *MultiSphinx* message format, which allows restricted multicast through designated mix nodes. Further optimisations to the scheme are briefly discussed in Section 5.5.

## 5.1 Detailed Construction

The Rollercoaster scheme is built upon the concept of a *schedule*. This schedule is derived deterministically from the source  $s$ , the total set of recipients  $U_{recv}$ , and the maximum branching factor  $k$  following Algorithm 1. First, a list  $U$  of all group members is constructed with the initial source at the 0-th index. The group size  $|U|$  and branching factor  $k$  lead to a total of  $\lceil \log_{k+1} |U| \rceil$  levels. In the  $t$ -th level the first  $(k + 1)^t$  members have already received the message. All of them send the message to the next  $w$  recipients, increasing the next group of senders to  $(k + 1)^{t+1}$ . In the 0-th level only  $U[0]$  (the initial sender) sends  $k$  messages to  $U[1] \dots U[k]$ .

**Algorithm 1** The basic Rollercoaster schedule algorithm for a given initial source  $s$ , list of recipients  $U_{recv}$ , and branching factor  $k$ . The *schedule* contains a list for every level with a tuple (*sender*, *recipient*) for each message to be sent.

```

1: procedure GENSCHEDULE( $s, U_{recv}, k$ )
2:    $U \leftarrow [s] + U_{recv}$ 
3:    $L \leftarrow \lceil \log_{k+1} |U| \rceil$  ▷ number of levels
4:    $schedule \leftarrow []$ 
5:   for  $t = 0$  until  $L - 1$  do
6:      $p \leftarrow (k + 1)^t$  ▷ first new recipient
7:      $w \leftarrow \min(k \cdot p, |U| - p)$ 
8:      $R \leftarrow []$ 
9:     for  $i = 0$  until  $w - 1$  do
10:       $idx_{sender} \leftarrow \lfloor \frac{i}{k} \rfloor$ 
11:       $idx_{recipient} \leftarrow p + i$ 
12:       $R[i] \leftarrow (U[idx_{sender}], U[idx_{recipient}])$ 
13:      $schedule[t] \leftarrow R$ 
14:   return  $schedule$ 

```

In order to associate an incoming message with the correct source node and group of all recipients, all Rollercoaster payloads contain a 16 byte header as illustrated in Figure 3, in addition to the *Sphinx* packet header used by Loopix. Each group is identified by a 32-bit *groupid* shared by all group members. The 32-bit *nonce* identifies previously received messages, which becomes relevant with fault-tolerance (Section 5.2). The fields *source*, *sender*, and *role* refer to individual group members and have a 10-bit size, allowing groups with up to 1024 members. The *source* field indicates the original sender and is necessary to construct the distribution graph at the recipient. The fields *sender* and *role* are used by the fault tolerant variant in Section 5.2 for acknowledgement messages and to route around nodes that are offline. Field lengths can easily be increased or decreased as they do not have to be globally the same across all Loopix clients. Finally, the header contains a signature that is generated by the original source and covers the payload as well as all static header fields. It assures recipients that the message indeed originated from a legitimate group member and that they are not tricked by an adversary to start distributing a fake message to group

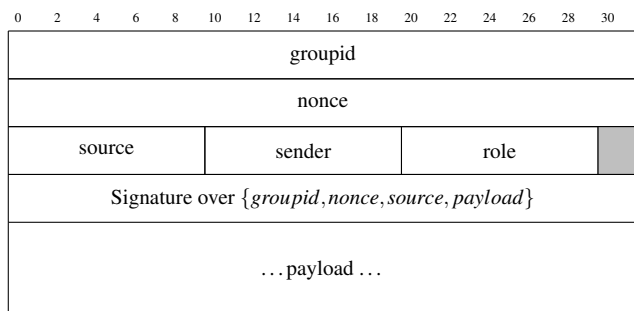


Figure 3: Payload header for the Rollercoaster scheme containing both the fields for the minimal scheme and the fields necessary for the fault-tolerance variant and further optimisations.

members. The *sender* and *role* fields are not covered by the signature, allowing nodes that are not the original source to modify these fields without invalidating the signature.

## 5.2 Adding Fault Tolerance

The basic Rollercoaster scheme of Section 5.1 fails when users are offline and cannot perform their role of forwarding messages. In this case, one or more recipients in later levels would not receive the message until their parent node returns online. The risk of this approach becomes apparent when looking at the graph in Figure 2B, where a single unavailable node causes message loss for its entire subtree. In principle, the responsibility for forwarding messages could be delegated to the provider nodes, which are assumed to always be online. However, we consider this approach not to be desirable as the adversary could learn about the group membership by compromising a provider.

*Rollercoaster with fault-tolerance* achieves reliable delivery through *acknowledgement* (ACK) replies to the source and reassignment of roles. When the source sends a message it sets timeouts by which time it expects an acknowledgement from the recipient and each of its children. The individual timeouts account for the number of hops and the expected delays at each hop due to mix node delays and messages waiting in send queues. ACKs are sent through the mix network like any other unicast message. When receiving an ACK from a node, the source marks the sending node as delivered. Choosing the source as the main coordinator is reasonable as it has the strongest incentive for ensuring delivery of all messages. Loopix allows a high rate of messages received by users, so it is not a problem if one user receives a large number of ACKs.

The source responds to a timeout by sending the message to a different node. For this, each node maintains a list of most-recently-seen nodes based on received messages and chooses one from it heuristically. The source itself is part of that list as the ultimate replacement node. A replacement

node is only necessary when the failing node would have forwarded the message to others, i.e. when it is not a leaf node of the distribution tree (see Algorithm 10 in Appendix B). Independently of this and in case that the message did not reach the intended recipient due to message loss, a *retry message* is sent (with exponential back-off) to the failed node again with its own timeout.

We start the timeouts associated with a message when the underlying Loopix implementation sends the message to the provider, so that the timeouts do not need to include the sender's queuing delay. Since the sender knows the global rate parameters  $\lambda_p$  and  $\lambda_\mu$ , it takes these into account when determining timeouts. The timeout may further be adjusted based on the network configuration and application requirements.

The fault-tolerance mechanism makes use of the message fields *source*, *sender*, and *role* shown in Figure 3. The *source* field remains unchanged as the message is forwarded because it is required for constructing the schedule at each node. It also indicates the node to which the ACK should be sent. The *sender* field is updated when forwarding a message or sending an ACK and used by the recipient to update their list of most-recently-seen nodes. The *role* field indicates the role that the receiving node should perform, usually their natural identity. However, when a node is offline, another node might be assigned its role, i.e. its position in the distribution tree. In this case, the role field indicates the node as which the recipient should act. Retry messages to failed nodes have an empty role field, because the role has already been reassigned.

On receiving any payload message *msg*, the recipient node hands over the payload to the application and reconstructs the schedule using *msg.source*, *msg.groupid*, and *msg.nonce*. For every child node of *msg.role* in the schedule, the node enqueues a message for the respective recipient, making sure to update *msg.role*. The ACK reply is enqueued after the payload messages so that no ACK is sent if a node goes offline before forwarding a message to all of its children in the distribution tree.

ACK messages contain the *groupid*, *nonce*, *source*, and *role* fields of the original message and an updated *sender* field, which allow the recipient of the ACK (i.e., the source) to identify and cancel the corresponding timeout. The sender adds a signature covering *all* header fields to ensure that the ACK message cannot be forged. When an ACK is not received on time, the message is sent to a different node as described above.

If the connection between a user and their provider is interrupted, we rely on the fact that Loopix allows users to retrieve received messages from their inbox later. The user's software notices a loss of connection and pauses timeouts until it has had a chance to check the inbox on the provider again.

After a long offline period, a node's inbox may contain a large backlog of messages that were received by the provider while the user was offline. When a node comes back online, it treats this backlog differently from messages received while

online: for any messages received while offline, a node only delivers the payloads to the application, but it does not send ACK messages or forward messages to other nodes. Here the node avoids doing unnecessary work for messages where the timeout is likely to have already expired.

Algorithm 8 in Appendix B describes the behaviour of the fault-tolerant variant in detail.

### 5.2.1 Eventual Delivery and Byzantine Fault Tolerance

The fault-tolerant variant of Rollercoaster assumes that the source node acts honestly and does not disconnect permanently (but can do so intermittently). This is reasonable as the sending user has high incentive to see through the delivery of their message. We prove eventual delivery under this assumption in the extended paper (see Appendix C). An application might provide the user with a suitable user interface that shows the delivery process.

*Proof sketch:* Everyone who does not ACK the payload will eventually receive it directly from the source, and will read it from their inbox when they return online. This works even in the presence of malicious nodes that acknowledge a message without forwarding it, since the source has individual timeouts for each group member. Therefore, the source will detect when a node’s children do not send ACKs.

However, the source node might be disconnected permanently. To nevertheless guarantee eventual delivery, every group member can periodically pick another group member at random and send it a hash of the message history it has seen so far (ordered in a deterministic way so that two users with the same set of messages obtain the same hash). If the recipient does not recognise the hash, the users run a reconciliation protocol [14] to exchange any messages that are known to only one of the users. Such a protocol provably guarantees that every user eventually receives every message, even if some of the users are Byzantine-faulty, provided that every user eventually exchanges hashes with every other user [14].

## 5.3 Exploring Delay and Traffic

We first analyse the expected multicast latency of Rollercoaster without fault tolerance by considering the levels of the distribution tree, as illustrated in Figure 2. The expected multicast latency  $D_{rollercoaster}$  is determined by the longest message forwarding paths  $C_1, C_2, \dots$ . Each such path is defined as  $C = e_0, \dots, e_{|C|-1}$  where  $e_i$  is an edge from a node on level  $i$  to a node on level  $i + 1$ . We call these edges *one-level edges*. The number of levels of the schedule generated by Algorithm 1 is  $L = \lceil \log_{k+1} |U| \rceil$  as discussed in §5.1. Hence, no path is longer than  $L$ . An example of a longest path is  $C = (a, b)(b, g)$  in Figure 2. The mean message delay when traversing each edge of the graph is  $\bar{d}_{msg} = \bar{d}_Q + \bar{d}_t$ , where  $\bar{d}_Q$  is the mean queuing delay and  $\bar{d}_t = \bar{d}_p + (l + 1) \cdot \bar{d}_\mu + \bar{d}_{pull}$  is the message’s mean travel time through the network, as in (2).

Scheme	Latency $D$	Packet size overhead
Naïve Unicast	$\mathcal{O}(m)$	–
Naïve Multicast	$\mathcal{O}(1)$	$\mathcal{O}(m)$
Rollercoaster	$\mathcal{O}(\log m)$	$\mathcal{O}(1)$

Table 2: Overhead of the presented multicast schemes in terms of group multicast delay and packet size overhead.

Since each node sends no more than a total of  $k$  messages to the directly subsequent level, the expected queuing delay for the last message is  $\bar{d}_Q = \frac{k-1}{\lambda_p}$ .

However, there are also edges from a node on level  $i$  to a node on level  $i + j$  where  $j > 1$ . One example is  $(a, d)$  in Figure 2. Messages from level  $i$  to level  $i + 1$  are sent before any messages that skip levels, and therefore any level-skipping messages may experience higher queuing delay before they are sent. Concretely, the edges from level  $i$  to level  $i + j$  will incur an additional expected queuing delay of at most  $(j - 1) \cdot \bar{d}_Q$  compared to one-level edges. At the same time, these edges save  $j - 1$  hops, which would have incurred both a queuing delay  $\bar{d}_Q$  and a travel time  $\bar{d}_t$  each. Hence, the time saved by the reduced hop count outweighs the extra queuing delay.

Thus, the expected time for a message to be received by all nodes is determined by the longest path consisting of only one-level edges, with a queuing delay of  $\bar{d}_Q = \frac{k-1}{\lambda_p}$  at each hop:

$$D_{rollercoaster} = L \cdot (\bar{d}_Q + \bar{d}_t) = \lceil \log_{k+1} m \rceil \cdot \bar{d}_{msg} \quad (6)$$

Hence, the group multicast latency is logarithmically dependent on the group size  $m$  and contains a multiplicative factor that equals the time to send a single message after being queued behind at most  $k$  messages.

When a node is offline, it will only be able to receive messages when it comes online and queries its inbox. In case the offline node is a forwarding node, the source will detect the lack of an ACK after the timeout expired. In this case the latency penalty for the children of the failed node is the timeout of the parent node, which is typically proportional to the expected delivery time.

## 5.4 p-Restricted Multicast with MultiSphinx

As specified so far, Rollercoaster uses the unmodified Loopix protocol. However, even though Rollercoaster spreads the work of sending a multicast message more evenly across the network than sequential unicast, payload messages and ACKs are still demanding for nodes’ send queues.

In this section, we consider a modification to the Loopix protocol that further improves multicast performance: namely, we allow some mix nodes to *multiply* one input message into

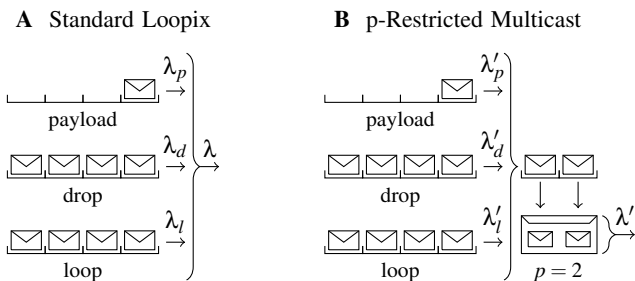


Figure 4: Standard Loopix (A) sends out a message if any of its Poisson processes triggers, so the rate of messages sent is  $\lambda = \lambda_p + \lambda_d + \lambda_l$ . In  $p$ -restricted multicast (B) these Poisson processes are still independent, but the node has an extra layer that awaits  $p$  messages, which are then wrapped into a MultiSphinx message. The sender can increase  $\lambda'_p$  to  $p\lambda_p$  (same for  $\lambda'_d, \lambda'_l$ ) while keeping  $\lambda' = \lambda$ .

multiple output messages, which may be sent to different recipients. The naïve mix-multicast we considered in Section 4.2 allows arbitrary multiplication factors. Here we show how to make mix-node-supported multicast safe by restricting the multiplication factor to a fixed constant  $p$ . We call this approach *p-restricted multicast* where clients can send  $p$  messages inside one MultiSphinx package; with  $p = 1$  this scheme is identical to the regular Rollercoaster.

In  $p$ -restricted multicast, only mix nodes in one designated layer may multiply messages. In our design, we perform multiplication in the middle layer (layer 2 of 3) and we refer to these mix nodes as *multiplication nodes*. To ensure unlinkability of mix nodes' inputs and outputs, every message processed by a multiplication node must result in  $p$  output messages, regardless of the message type or destination. Mix nodes in other layers retain the standard one-in-one-out behaviour of Loopix. Since layer 3 of the mix network needs to process  $p$  times as many messages as the earlier layers, layer 3 should contain  $p$  times as many mix nodes as layers 2.

This paper uses the parameter  $p$  for  $p$ -restricted multicast and  $k$  for the schedule algorithm. These can be chosen independently of each other. However, for simplicity and practical interdependence we often set both to the same value  $k = p$ .

Effectively,  $p$ -restricted multicast allows  $p$  messages to different recipients to be packaged as a single message up to  $p$  times the size. Sending fewer but larger messages allows for lower power consumption on mobile devices, as discussed in our application requirements (§2). We show in our evaluation in §6.5 that  $p$ -restricted multicast allows choosing much larger  $\lambda$  values while maintaining low latency.

#### 5.4.1 The MultiSphinx message format

Loopix encodes all messages using the *Sphinx* message format [11], which consists of a header  $M$  containing all metadata

and an encrypted payload  $\delta$ . Using the header, each mix node  $n_i$  derives a secret shared key  $s_i$ . Due to the layered encryption of the header and payload, an adversary cannot correlate incoming and outgoing packets when observing mix nodes. Our construction is based on the improved Sphinx packet format [15] which uses authenticated encryption (AE). In particular, we use a stream cipher  $C$  in an encrypt-then-MAC regime and require that without the knowledge of the key, the generated ciphertext is indistinguishable from random noise (which is believed to be the case for modern ciphers such as AES-CTR). Every hop verifies integrity of the entire message to prevent active tagging attacks. The improved Sphinx packet format satisfies the ideal functionality of Sphinx [16]. The per-hop integrity checks of the entire message come at the cost of lacking support for anonymous reply messages, but these are not used by Loopix.

Sphinx assumes that each input message to a mix node results in exactly one output message. In order to support  $p$ -restricted multicast we introduce the *MultiSphinx* message format, which can wrap  $p$  messages. A MultiSphinx message is unwrapped at a designated mix node, and split into  $p$  independent messages. For anyone other than the designated multiplication node, MultiSphinx messages are indistinguishable from regular Sphinx packets. We now describe the *MultiSphinx* design for  $p = 2$  by describing the creation and processing of these messages. The detailed construction and processing is formalised in Appendix A.2.

For  $p = 2$ , the sender waits until its message queues (payload, drop, loop) have released two messages. The sender then combines their payloads  $\delta_A, \delta_B$  and recipients  $U_A, U_B$  into a single message that is inserted into the mix network, as shown in Figure 4. As we want to fit both payloads and two headers into our message to the multiplication node,  $|\delta_A|$  and  $|\delta_B|$  must be smaller than the global Sphinx payload size.

The combined message is sent via a mix node  $n_0$  in the first layer to the designated multiplication node  $n_1$ , where its inner messages are extracted and added to its input buffer. The inner message containing  $\delta_A$  will be processed by  $n_1$  and routed via  $n_{2,A}$  to the recipient  $n_A$  (and similarly for B). The multiplication node derives the secret key  $s_1$  from the incoming message's header and additional secret keys  $s_{1,A}, s_{1,B}$  from the headers of the inner messages. We omit provider nodes.

The sender first computes all secret keys. Using these secret keys it encrypts the payloads  $\delta_A, \delta_B$  between the recipients and the multiplication node. However, the resulting encrypted payloads are smaller than the regular Sphinx payload lengths.

To ensure all messages have the same size, we use a pseudo-random function (PRF, e.g. HMAC)  $\rho$  to add padding to the encrypted payloads  $\delta_{1,A}$  and  $\delta_{1,B}$ .  $\rho$  is keyed with the shared secret  $s_1$  and the payload index (A or B) so that the padding is unique. The resulting payloads have the format  $\delta'_{1,A} = \delta_{1,A} \parallel \rho(s_1 \parallel A)$  (and similarly for B). Now the sender computes the headers and MACs along the path from the multiplication node to the recipients by simulating the decrypt-

tion of the payload at each step. This results in two Sphinx headers  $M_{1,A}$  and  $M_{1,B}$ . Finally, we create the message for the path from the sender to the multiplication node using the regular Sphinx construction. We set the payload of that message to the concatenation  $\delta_{combined} = M_{1,A} \parallel \delta_{1,A} \parallel M_{1,B} \parallel \delta_{1,B}$ . Appendix A.2 contains pseudocode for this construction.

The processing of incoming messages at the multiplication node differs from other nodes. First, the payload is decrypted and split into the message headers and payloads. Then, the payloads are deterministically padded using the PRF  $\rho$  as described above. To ensure that the messages are hard to correlate, they are added to the node's input buffer, decrypted again (now deriving secrets  $s_{1,\{A,B\}}$ ), and delayed independently as defined by their individual delay parameter.

### 5.4.2 Anonymity of MultiSphinx

All MultiSphinx messages (before and after the multiplication node) have the same header length and payload length as regular Sphinx messages. Sphinx headers do not leak the number of remaining hops and the ciphertext is indistinguishable from random noise. Therefore, MultiSphinx messages are indistinguishable from regular Loopix messages. At the same time, the multiplication node maintains the unlinkability between the incoming messages and outgoing messages as these are delayed independently.

An adversary might also corrupt mix nodes. Even in this case they do not gain advantage over regular Sphinx message with regards to sender and recipient anonymity and unlinkability. These results also hold for active adversaries with the capabilities from the original Loopix paper.

If an adversary controls a  $p$ -restricted multiplication node and  $c_3$  of the  $n_3$  mix nodes of the third layer, they can trace some messages from their multiplication to their delivery at providers. On the basis that the  $p$  recipients of a MultiSphinx message are likely to be members of the same group, the adversary then has a chance to guess that any two of the users from these providers share a group membership. The probability of correctly guessing two group members given a group message is less than  $(1 - (\frac{n_3 - c_3}{n_3})^{p-1}) \cdot \frac{|\mathcal{P}|^2}{|\mathcal{U}|^2}$  if all  $|\mathcal{U}|$  users are evenly distributed among  $|\mathcal{P}|$  providers. This attack is prevented if the multiplication node *or* all but one of the chosen nodes in the third layer are trustworthy. (In contrast, standard Loopix requires only that any mix node on the message path is trustworthy.) MultiSphinx does not leak any information regarding group sizes. The extended paper (see Appendix C) contains theorems and proofs for our claims.

In addition to these properties, it is possible to achieve sender anonymity by first forwarding the message to a trusted group member. The sender can prove its membership through a shared group secret. We leave receiver anonymity and unlinkable group membership for future work.

## 5.5 Further Optimisations

The schedule computed by GENSCHEDULE in Algorithm 1 delivers the first messages to the nodes at the beginning of the provided recipient list  $U_{recv}$ . These nodes will always act as the forwarding nodes. To better balance these among all group members, one can shuffle the list based on a *nonce* value that is part of the message. This variant is described in Algorithm 2. As the GENSCHEDULERAND algorithm is still deterministic and the nonce is part of the Rollercoaster header, each node reconstructs the same schedule.

---

**Algorithm 2** Creating a pseudorandomized schedule for a given nonce

---

```

1: procedure GENSCHEDULERAND( $s, U_{recv}, k, nonce$ )
2:    $R \leftarrow \text{NEWPRNG}(nonce)$ 
3:    $U'_{recv} \leftarrow \text{R.shuffle}(U_{recv})$ 
4:   return GENSCHEDULE( $s, U'_{recv}, k$ )

```

---

Further optimisation is possible if different sub-groups display different levels of activity and connectivity. For example, if there is a small, active sub-group communicating while the rest of the group remains passive, it is more important for messages to travel faster between active nodes to support swift, effective collaboration. Active nodes can often be assumed to be more likely to be online. Agreeing on the full order is no longer possible through a single nonce value. However, the source can randomly compute a subset of all schedules, evaluate the generated schedule against its information about the group members, and choose one that creates a schedule with the most desirable properties.

## 6 Evaluation

For the empirical evaluation we developed a mix network simulation tool that provides fully reproducible results. First, we discuss the behaviour and results of the Rollercoaster scheme in an ideal scenario where all participants are online throughout. Second, we discuss the impact of offline nodes and how this is addressed by the fault-tolerant variant of Rollercoaster. Finally, we discuss the impact of multi-group membership, sending multiple messages at once, and  $p$ -restricted multicast.

### 6.1 Methodology

Since the real-world performance of Loopix has been practically demonstrated [3] we run a simulation instead of an experiment on a real network. This provides clear practical advantages: First, it allows us to eliminate external influences such as network congestion due to unrelated traffic or CPU usage by other processes. Second, the simulated time can run faster than real-time, allowing us to gather significantly more results using less computational resources. Third, it makes monitoring and categorising traffic easier as packets and node

state can be inspected. Finally, by initialising the PRNG with a fixed seed, the results of this paper are fully reproducible.

The simulator runs the entire mix network on a single machine, with nodes communicating through shared memory simulating a network. It instantiates objects for each participating user, provider, and mix node. All objects implement a `tick()` method in which they process incoming messages and mimic the designed node behaviour such as delaying and forwarding packets. As we are primarily interested in the traffic behaviour, no actual encryption is performed. The original Loopix paper has shown that the queuing time and per-hop delays dominate the message delay, and that CPU time for cryptographic operations is insignificant in comparison. Similarly, the network delay is negligible.

For the final evaluation we ran 276 independent simulations, covering more than 992,160 hours of simulated node time in less than 209 hours of CPU core time. This is a relative speed up by factor  $4500\times$  compared to a real network experiment of the same scope. In every simulation step the application (see below) measures the message latency  $d_{msg}$  of each delivered message between the original source and each recipient. We verified that our simulator behaves faithfully to the Loopix implementation by reproducing a latency distribution graph from the original paper [3, Figure 11]. Our simulator is implemented in less than 2,000 lines of Python code including tests and is available as an open-source project.<sup>2</sup>

The network simulator assigns 16 users to each provider. We set the Loopix rates  $\lambda_p = \lambda_d = \lambda_l = 2/s$  for the client nodes and the delay rate  $\lambda_u = 3/s$ . Hence, the overall sending rate of the clients is  $\lambda = 6/s$ . This meets the requirement  $\lambda/\lambda_u \geq 2$  that is suggested by the Loopix paper [3, p. 1209,  $\lambda_u = \mu$ ]. The mix network consists of 3 layers containing 3 mix nodes each (mix loop injection rate  $\lambda_M = 2/s$ ). All simulations are run with a granularity of 10ms per tick. The simulated time span for all configurations is 24h.

The application behaviour is modelled by a Poisson process. On average every 30s one of the online nodes sends a single message to all other group members. We account for participation inequality [8] by dividing the group using an 80/20 rule: 20% of users in the group send 80% of all messages, and vice versa.

## 6.2 Results with All Users Online

For a group of size 128, the average latency is reduced from 34.9s in sequential unicast to 7.0s (8.3s for group size 256) in Rollercoaster with  $k = p = 2$ . This fulfils our application requirements that were derived from the user study concerning delay in collaborative applications [7]. The results are compatible with our analytical results as discussed in Section 5.3. For Rollercoaster not only is the average latency low, but most of the latency distribution falls within fairly tight bounds – that is, very large latencies are rare. Figure 5 shows

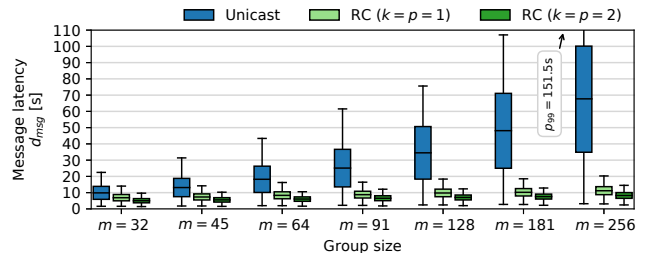


Figure 5: This box plot shows the distributions of message latency  $d_{msg}$  for increasing group sizes for the strategies *naive sequential unicast* and *Rollercoaster (RC)*. The Rollercoaster strategies show different  $k$  and  $p$  parameters. The boxes span from the first quartile to the third quartile (middle line is the median) and the whiskers indicate the 1st and 99th percentile.

the latency achieved by the Rollercoaster scheme with and without  $p$ -restricted multicast for different percentiles and compares them to unicast. For a group with 128 members the 99th percentile  $p_{99}$  for Rollercoaster is 12.3s ( $p_{90}$ : 9.9s) whereas in unicast it is 75.6s ( $p_{90}$ : 60.8s). We provide detailed histograms in the extended paper (see Appendix C).

## 6.3 Results for Fault-Tolerance Scenarios

The evaluation of the fault tolerance properties requires a realistic model of connectivity of mobile devices. For this we processed data from the *Device Analyzer* project [17] that contains usage data of volunteers who installed the Android app. The online/offline state of a device is derived from its trace information regarding network state, signal strength, and airplane mode. We limit the dataset ( $n = 27790$ ) to traces that contain connectivity information ( $n = 25618$ ), cover at least 48 hours ( $n = 20117$ ), and have no interval larger than 12 hours without any data ( $n = 2772$ ).

Inspecting the traces we identify three archetypes of online behaviour. The first group is online most of the time and is only interrupted by shorter offline segments of less than 60 minutes. Members of the second group have at least one large online segment of  $> 8$  hours and are on average online 50% or more of the time. Finally, the third group is online less than 50% of the time with many frequent changes between online and offline states. As the dataset is more than five years old we decided to use the characteristics of these groups to build a model. Using a model allows us to extrapolate offline behaviour into scenarios with increased connectivity. In the model following the parameters of the original dataset, the fraction of all users' time spent online is 65%. In a second and third model with increased connectivity, we increase this percentage to 80% and 88%, respectively, while preserving the behaviour of the archetype groups. The generated models are visualised in the extended paper (see Appendix C).

<sup>2</sup><https://github.com/lambdapioneer/rollercoaster>

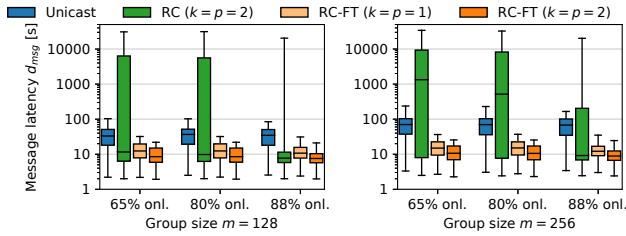


Figure 6: The distribution of message latency  $d_{msg}$  for different offline scenarios. From left to right the strategies are Unicast, Rollercoaster without fault-tolerance (RC), and Rollercoaster with fault-tolerance (RC-FT). Boxes and whiskers as in Figure 5.

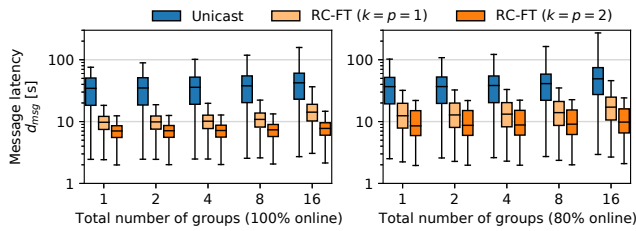


Figure 7: Message latency  $d_{msg}$  for an increasing number of groups for 128 users (every user is member of every group). Boxes and whiskers as in Figure 5.

For our discussion of offline behaviour we refine our previous definition of message latency  $d_{msg}$ : we ignore all latencies where the intended recipient was offline when the message was placed into their inbox by the provider node. This change has the practical benefit of excluding outliers. More importantly, fast delivery to an offline user has no real-world benefit. Instead, a good multicast algorithm should optimise the delivery to all nodes that are active and can actually process an incoming message. The source might go offline at any time regardless of outstanding messages.

Without fault tolerance, the presence of offline nodes greatly increases the 99th percentile ( $p_{99}$ ) for Rollercoaster (RC) to more than 10,000s for a group of 128 members. The fault-tolerant variant (RC-FT) reduces the 99th percentile to less than 21.9s ( $p_{90}$ : 18.0s). In unicast  $p_{99}$  latency is 103.3s ( $p_{90}$ : 61.9s). Figure 6 shows that the fault-tolerant variant generally outperforms unicast at various percentiles. We provide detailed histograms in the extended paper (see Appendix C).

### 6.4 Multiple Groups and Message Bursts

Users might be part of multiple groups, which increases their burden of distributing messages. In this evaluation we assign 128 users to a growing number of groups. Figure 7 shows that the number of group memberships has little impact on Rollercoaster’s performance both for online and offline scenarios.

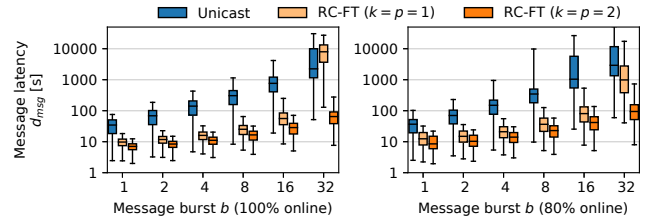


Figure 8: Message latency  $d_{msg}$  for applications that send  $b$  messages at once. The group size is  $m = 128$ . Boxes and whiskers as in Figure 5.

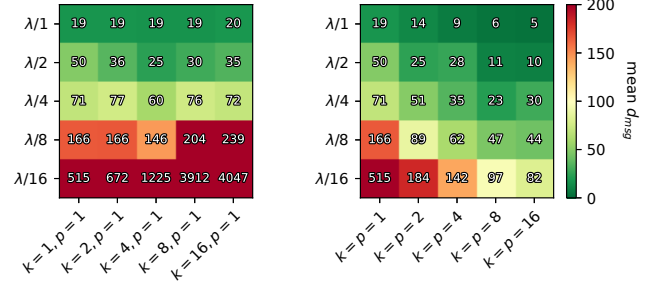


Figure 9: Heatmaps showing the mean message latency for reduced sending rates (y-axis) and different Rollercoaster parameters (x-axis). In the left graph only the logical branch factor  $k$  is increased. In the right graph the multicast factor  $p$  is increased at the same time. Group size is  $m = 128$  and 80% online.

Similarly, users might be sharing large payloads (e.g. images) or sending multiple updates at once. Both translate into many messages being scheduled for distribution at the same time, which risks overwhelming the payload queue. Figure 8 shows that Rollercoaster can handle many more messages sent in bursts than unicast. We observed that with unicast and some Rollercoaster configurations some nodes had indefinitely growing send buffers as the simulation progressed. The effect of this can be seen by the higher message latencies for  $b = 32$ . This threshold is higher for  $p$ -restricted multicast.

### 6.5 Results for p-Restricted Multicast

In this evaluation we show that  $p$ -restricted multicast allows us to drastically lower the sending rates  $\lambda_{\{p,d,l\}}$  of the clients while achieving similar performance. A low sending rate is desirable as it allows the radio network module to return to standby and thereby saving significant battery energy on mobile devices (see §2). Figure 9 shows that just increasing  $k$  (left) has negligible or even negative impact, while increasing  $k$  and  $p$  together (right) allows for lower sending rate  $\lambda$  while maintaining good enough performance. We decrease  $\lambda_{\mu}$  accordingly to maintain the  $\lambda/\lambda_{\mu} \geq 2$  balance (see §6.1) which increases the per-hop delays.

## 7 Related Work

Previous research on efficient anonymity networks achieves strong security goals, high efficiency, scalability, and offline support. However, decentralised low-latency group multicast while guaranteeing the strongest privacy guarantees against a global adversary has not yet received due attention.

Work based on *Dining Cryptographer networks (DC-nets)* [18] is inherently broadcast-based as the round results are shared with all nodes. These designs generally provide sender anonymity and impressive functionality. However, the required synchronisation and communication overhead render them unsuitable for low latency applications. As the rounds depend on the calculations of all clients, they can be susceptible to interference by malicious participants. The Xor-Trees by Dolev et al. [19] achieve efficient multicast, but only in the absence of an active attacker. Dissent [20] can provide protection against such active attacks. However, its design does not scale as well as Loopix due to its need to broadcast messages to all clients, and not just the intended group of recipients.

*Circuit-based onion routing* networks such as Tor [1] establish long-living paths through multiple hops. All messages from and to the client are transmitted via the same path with every node peeling off the outer-most encryption layer. They are arguably the most widely deployed and accessible class of anonymity network designs. While the onion path approach allows for low latency communication, it is known to be vulnerable against global adversaries performing *traffic analysis* attacks [2, 21]. Most mainstream designs consider one-to-one communication, but there is interesting work on building multicast trees using onion-routing techniques. Examples are AP3 [22], M2 [23], and MTor [24]. When facing a global adversary, they share similar vulnerabilities to Tor.

Multicast in friend-to-friend overlays as in VOUTE [25,26] share a similarity with our work as trusted peers help with message distribution. However, to our knowledge, there are no practical implementations with performance similar to Loopix. Using real-world trust relationships together with Rollercoaster for inter-group communication is an interesting direction for future work.

The recent Vuvuzela design [27] cleverly leverages dead drops and cover traffic to achieve strong metadata privacy while maintaining a high throughput of messages. Pursuing the goal of limiting network bandwidth use results in delays of up to 10 minutes to initiate a call and more than 30 seconds latency for messages, which we consider too large for many collaborative applications. Its privacy guarantees can be limited in the case of an active attacker with a priori suspicion of a certain group of users communicating.

Work based on *private information retrieval (PIR)* such as Pung [28] and Talek [29] allows for low-latency group communication with strong security guarantees. However, these systems are not decentralised and rely on the availability

of high-spec servers. Moreover, their latency scales with the total number of users  $n$  rather than the group sizes.

We note that our evaluation differs from the standard methods in similar papers [3, 20, 27] using real servers and networks. Since it is already established that the performance of Loopix is viable in practise, we can build on top of this and focus on more inspectable and reproducible evaluations through deterministic simulation.

The Shadow project [30] can simulate actual anonymity network implementations in a network topology on a single machine. With extensive modelling options the network and user behaviour can be modelled deterministically. However, since the application binaries remain black-boxes it cannot guarantee complete deterministic behaviour. White-box simulators such as Mixim [31] calculate the entropy as messages pass through the system.

Many multicast systems use distribution trees [32–36]. However, to our knowledge, these protocols have not yet been applied in the context of mix networks, where the limited send rate and artificial message delays introduce particular challenges not considered by existing multicast protocols.

## 8 Conclusion

In this paper we have presented an efficient scheme for multicast in mix networks named *Rollercoaster*. Compared to the sender of a message naïvely sending it to all other group members by unicast, our scheme significantly lowers the time until all group members receive the message. For a group of size  $m = 128$ , Rollercoaster is faster by a factor of 5, reducing the average delay from 34.9s to 7.0s and reducing the 99th percentile from 75.6s to 12.3s. We do this by involving more users than just the original sender in the process of disseminating a message to group members. This also reduces the asymptotic growth of the expected delay to  $\mathcal{O}(\log m)$ . A key ingredient for this is the deterministic GENSCHEDULE algorithm that allows users to share plans for message distribution using a single nonce.

Faced with the challenge of unreliable and offline nodes, we have introduced a variant of our algorithm that allows acknowledgement and retry of message delivery as well as reassignment of tasks from offline to online users. In the failure-free case, it adds a constant message overhead that does not worsen the results measured. When nodes are offline it significantly improves reliability and delays.

Our simulation tool enabled us to obtain reproducible and inspectable performance measurements. The low cost of simulation enabled us to efficiently explore the behaviour of many system configurations with a large number of users.

In future work we plan to implement and run collaborative applications and group messaging protocols on a network using Rollercoaster. We also hope to extend Rollercoaster with facilities to add or remove members of a group.

## Acknowledgements

We thank Steven J. Murdoch, Killian Davitt, and our anonymous reviewers for the helpful discussions and their valuable input. Daniel Hugenroth is supported by a Nokia Bell Labs Scholarship and the Cambridge European Trust. Martin Kleppmann is supported by a Leverhulme Trust Early Career Fellowship, the Isaac Newton Trust, Nokia Bell Labs, and crowdfunding supporters including Ably, Adrià Arcarons, Chet Corcos, Macrometa, Mintter, David Pollak, RelationalAI, SoftwareMill, Talent Formation Network, and Adam Wiggins. Alastair R. Beresford is partially supported by EPSRC [grant number EP/M020320/1].

## References

- [1] R. Dingledine, N. Mathewson, and P. Syverson, “Tor: The second-generation onion router,” tech. rep., Naval Research Lab Washington DC, 2004.
- [2] S. J. Murdoch and G. Danezis, “Low-cost traffic analysis of Tor,” in *2005 IEEE Symposium on Security and Privacy*, pp. 183–195, IEEE, 2005.
- [3] A. M. Piotrowska, J. Hayes, T. Elahi, S. Meiser, and G. Danezis, “The Loopix anonymity system,” in *26th USENIX Security Symposium*, pp. 1199–1216, 2017.
- [4] M. Kleppmann, S. A. Kollmann, D. A. Vasile, and A. R. Beresford, “From secure messaging to secure collaboration,” in *26th International Workshop on Security Protocols*, pp. 179–185, Springer, 2018.
- [5] M. Ahmed-Nacer, C.-L. Ignat, G. Oster, H.-G. Roh, and P. Urso, “Evaluating CRDTs for real-time document editing,” in *11th ACM Symposium on Document Engineering*, pp. 103–112, ACM, Sept. 2011.
- [6] A. Pfitzmann and M. Hansen, “A terminology for talking about privacy by data minimization: Anonymity, unlinkability, undetectability, unobservability, pseudonymity, and identity management,” Aug. 2010. v0.34, [http://dud.inf.tu-dresden.de/literatur/Anon\\_Terminology\\_v0.34.pdf](http://dud.inf.tu-dresden.de/literatur/Anon_Terminology_v0.34.pdf).
- [7] C.-L. Ignat, G. Oster, O. Fox, V. L. Shalin, and F. Charoy, “How do user groups cope with delay in real-time collaborative note taking,” in *14th European Conference on Computer Supported Cooperative Work*, pp. 223–242, Springer, Sept. 2015.
- [8] J. Nielsen, “The 90-9-1 rule for participation inequality in social media and online communities,” 2006. <https://www.nngroup.com/articles/participation-inequality/>.
- [9] J. Huang, F. Qian, A. Gerber, Z. M. Mao, S. Sen, and O. Spatscheck, “A close examination of performance and power characteristics of 4G LTE networks,” in *10th International Conference on Mobile Systems, Applications, and Services*, pp. 225–238, 2012.
- [10] D. Chaum, “Untraceable electronic mail, return addresses, and digital pseudonyms,” *Communications of the ACM*, vol. 24, no. 2, 1981.
- [11] G. Danezis and I. Goldberg, “Sphinx: A compact and provably secure mix format,” in *30th IEEE Symposium on Security and Privacy*, pp. 269–282, IEEE, 2009.
- [12] A. Serjantov, R. Dingledine, and P. Syverson, “From a trickle to a flood: Active attacks on several mix types,” in *International Workshop on Information Hiding*, pp. 36–52, Springer, 2002.
- [13] S. Deering, “Host extensions for IP multicasting,” STD 5, RFC Editor, August 1989. <http://www.rfc-editor.org/rfc/rfc1112.txt>.
- [14] M. Kleppmann and H. Howard, “Byzantine eventual consistency and the fundamental limits of peer-to-peer databases,” *arXiv preprint arXiv:2012.00472*, 2020.
- [15] F. Beato, K. Halunen, and B. Mennink, “Improving the Sphinx mix network,” in *International Conference on Cryptology and Network Security*, pp. 681–691, Springer, 2016.
- [16] C. Kuhn, M. Beck, and T. Strufe, “Breaking and (partially) fixing provably secure onion routing,” *arXiv preprint arXiv:1910.13772*, 2019.
- [17] D. T. Wagner, A. Rice, and A. R. Beresford, “Device analyzer: Understanding smartphone usage,” in *International Conference on Mobile and Ubiquitous Systems: Computing, Networking, and Services*, pp. 195–208, Springer, 2013.
- [18] D. Chaum, “Security without identification: Transaction systems to make Big Brother obsolete,” *Communications of the ACM*, vol. 28, no. 10, pp. 1030–1044, 1985.
- [19] S. Dolev and R. Ostrobsky, “Xor-trees for efficient anonymous multicast and reception,” *ACM Transactions on Information and System Security*, vol. 3, no. 2, pp. 63–84, 2000.
- [20] D. I. Wolinsky, H. Corrigan-Gibbs, B. Ford, and A. Johnson, “Dissent in numbers: Making strong anonymity scale,” in *10th USENIX Symposium on Operating Systems Design and Implementation*, pp. 179–182, 2012.
- [21] G. Danezis and A. Serjantov, “Statistical disclosure or intersection attacks on anonymity systems,” in *International Workshop on Information Hiding*, pp. 293–308, Springer, 2004.

[22] A. Mislove, G. Oberoi, A. Post, C. Reis, P. Druschel, and D. S. Wallach, “AP3: Cooperative, decentralized anonymous communication,” in *11th ACM SIGOPS European workshop*, p. 30, ACM, 2004.

[23] G. Perng, M. K. Reiter, and C. Wang, “M2: Multicasting mixes for efficient and anonymous communication,” in *26th IEEE International Conference on Distributed Computing Systems*, pp. 59–59, IEEE, 2006.

[24] D. Lin, M. Sherr, and B. T. Loo, “Scalable and anonymous group communication with MTor,” *Proceedings on Privacy Enhancing Technologies*, vol. 2016, no. 2, pp. 22–39, 2016.

[25] S. Roos, M. Beck, and T. Strufe, “Anonymous addresses for efficient and resilient routing in F2F overlays,” in *35th Annual IEEE International Conference on Computer Communications*, pp. 1–9, IEEE, 2016.

[26] S. Roos, M. Beck, and T. Strufe, “Voute-virtual overlays using tree embeddings,” *arXiv preprint arXiv:1601.06119*, 2016.

[27] J. Van Den Hooff, D. Lazar, M. Zaharia, and N. Zeldovich, “Vuvuzela: Scalable private messaging resistant to traffic analysis,” in *25th Symposium on Operating Systems Principles*, pp. 137–152, 2015.

[28] S. Angel and S. Setty, “Unobservable communication over fully untrusted infrastructure,” in *12th USENIX Symposium on Operating Systems Design and Implementation*, pp. 551–569, 2016.

[29] R. Cheng, W. Scott, E. Masserova, I. Zhang, V. Goyal, T. Anderson, A. Krishnamurthy, and B. Parno, “Talek: Private group messaging with hidden access patterns,” *arXiv preprint arXiv:2001.08250*, 2020.

[30] R. Jansen and N. Hopper, “Shadow: Running Tor in a box for accurate and efficient experimentation,” in *19th Symposium on Network and Distributed System Security*, Internet Society, February 2012.

[31] I. B. Guirat, D. Gosain, and C. Diaz, “Mixim: A general purpose simulator for mixnet,” *Privacy Enhancing Technologies Symposium – HotPETs Workshop*, 2020.

[32] M. Hosseini, D. T. Ahmed, S. Shirmohammadi, and N. D. Georganas, “A survey of application-layer multicast protocols,” *IEEE Communications Surveys & Tutorials*, vol. 9, no. 3, pp. 58–74, 2007.

[33] A. Popescu, D. Constantinescu, D. Erman, and D. Ilie, “A survey of reliable multicast communication,” in *Conference on Next Generation Internet Networks, NGI*, pp. 111–118, IEEE, 2007.

[34] C. K. Yeo, B.-S. Lee, and M. H. Er, “A survey of application level multicast techniques,” *Computer Communications*, vol. 27, no. 15, pp. 1547–1568, 2004.

[35] J. Leitão, J. Pereira, and L. Rodrigues, “Epidemic broadcast trees,” in *26th IEEE International Symposium on Reliable Distributed Systems, SRDS 2007*, pp. 301–310, IEEE, Oct. 2007.

[36] J. Leitão, J. Pereira, and L. Rodrigues, “Gossip-based broadcast,” in *Handbook of Peer-to-Peer Networking*, pp. 831–860, Springer, Oct. 2009.

## A MultiSphinx Construction

In this Appendix we provide detailed algorithms for constructing and processing both the regular Sphinx messages (A.1) and our MultiSphinx messages (A.2). The regular construction is based on the original Sphinx paper [11] and the proposed improvement using authenticated encryption [15]. For both schemes we will use three hops  $n_0, n_1, n_2$  for the mix nodes and a final hop  $n$  for the recipient<sup>3</sup> that extracts the payload from the inner-most encryption (see Figure 10).

A Sphinx header  $M$  consists of a group element  $\alpha$  for deriving shared secrets, authenticated data  $\beta$ , and an authentication tag  $\gamma$ . In the original Sphinx paper  $\beta$  is used to store the address of the next hop. For the final hop the distinguished element  $*$  is used to signal that the payload reached its intended destination. Loopix adds per-hop delays to this routing information.

We assume that all nodes  $n_i$  have access to the public keys of all other nodes without us passing these explicitly. We assume the existence of a method `PROCESSHEADER` that takes a header of a Sphinx packet and returns all metadata contained in  $\beta$  (next hop identifier, delay) and the header for the next hop. We assume the existence of a method `COMPUTESECRETS` that takes a list of hops  $n_0, n_1, \dots$  and outputs

<sup>3</sup>We omit the provider nodes here to improve readability.

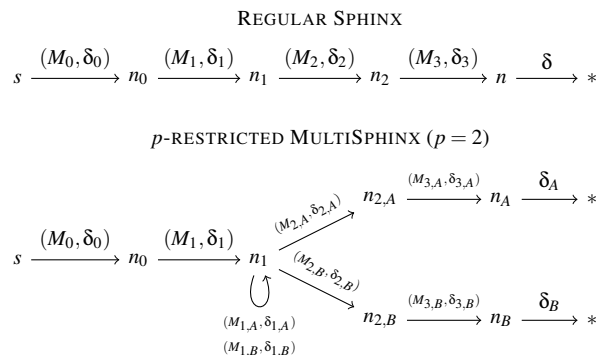


Figure 10: Schematic of messages (header, payload) for Sphinx and MultiSphinx.

a list of shared secrets  $s_0, s_1, \dots$ . We assume the existence of a method `CREATEHEADER` that takes a shared secret  $s_i$ , the next hop identifier  $n_{i+1}$ , and (optionally) a header  $M_{i+1}$  to wrap. The details of these operations can be found in the Sphinx paper [11, §3.2 and §3.6]. In line with Loopix the sender chooses a random per-hop delay for each hop and includes it in the authenticated metadata in the header. This happens transparently in the `CREATEHEADER` method.

We assume the existence of an authenticated encryption (AE) scheme as required by the improved Sphinx format [15]. An AE scheme provides an encryption function  $AE_{enc}$  that takes a secret key  $s$ , a message  $msg$ , and optional metadata  $meta$  and outputs a ciphertext  $ctext$  and an authentication tag  $auth$ . It also provides a decryption function  $AE_{dec}$  that takes a secret key  $s$ , a ciphertext  $ctext$ , an authentication tag  $auth$ , and metadata  $meta$ . It returns the decrypted message if the authentication tag verifies the integrity of ciphertext and metadata or  $\perp$  otherwise.

We assume that the AE scheme is based on an encrypt-then-mac regime using a stream cipher  $C$  (e.g. AES-CTR), a message authentication code MAC (e.g. HMAC), and a keyed key derivation function KDF (e.g. HKDF). Stream ciphers have the property that changing a given bit of the ciphertext/plaintext only changes the bit at the same position in the plaintext/ciphertext after decryption/encryption. Arbitrary changes will lead to an invalid auth tag – but we might intentionally ignore this during our constructions and recalculate the auth tags later. Since Sphinx uses fresh secret keys for every message and hop, we can leave the nonce for the stream cipher constant. We show our construction of  $AE_{enc}$  and  $AE_{dec}$  in Algorithm 3.

---

**Algorithm 3** The authenticated encryption scheme AE based on stream cipher  $C$ , a MAC, and a keyed KDF.

---

```

1: procedure  $AE_{enc}(s, msg, meta)$ 
2:    $s_{cipher}, s_{mac} \leftarrow KDF(s, cipher), KDF(s, mac)$ 
3:    $ctext \leftarrow C(s_{cipher}) \oplus msg$ 
4:    $auth \leftarrow MAC(s_{mac}, ctext \parallel meta)$ 
5:   return  $(ctext, auth)$ 
6:
7: procedure  $AE_{dec}(s, ctext, auth, meta)$ 
8:    $s_{cipher}, s_{mac} \leftarrow KDF(s, cipher), KDF(s, mac)$ 
9:   if  $MAC(s_{mac}, ctext \parallel meta) \neq auth$  then
10:    return  $\perp$ 
11:    $msg \leftarrow C(s_{cipher}) \oplus ctext$ 
12:   return  $msg$ 

```

---

## A.1 Normal Sphinx (existing solution)

The algorithms in this section summarise the existing literature [11, 15], but we have adapted the notation to be more concise. Algorithm 4 shows the creation of the a regular

Sphinx message by the sender. While the original Sphinx papers can create all headers before encrypting the payload, the improved variant with AE requires us to do these operations simultaneously as the encryption affects the authentication tag  $\gamma$  of this and the following message headers.

---

**Algorithm 4** Creating a packet to be routed through hops  $n_0, n_1, n_2$  to node  $n$ .

---

```

1: procedure  $CREATE(\delta, n_0, n_1, n_2, n)$ 
2:   assert  $|\delta| = MAXMSGLEN$ 
3:    $s_0, s_1, s_2, s_3 \leftarrow COMPUTESECRETS(n_0, n_1, n_2, n)$ 
4:    $M_3 \leftarrow CREATEHEADER(s_3, *)$ 
5:    $\delta_3, M_3.\gamma \leftarrow AE_{enc}(s_3, \delta, M_3.\beta)$ 
6:    $M_2 \leftarrow CREATEHEADER(s_2, n, M_3)$ 
7:    $\delta_2, M_2.\gamma \leftarrow AE_{enc}(s_2, \delta_3, M_2.\beta)$ 
8:    $M_1 \leftarrow CREATEHEADER(s_1, n_2, M_2)$ 
9:    $\delta_1, M_1.\gamma \leftarrow AE_{enc}(s_1, \delta_2, M_1.\beta)$ 
10:   $M_0 \leftarrow CREATEHEADER(s_0, n_1, M_1)$ 
11:   $\delta_0, M_0.\gamma \leftarrow AE_{enc}(s_0, \delta_1, M_0.\beta)$ 
12:  return  $(M_0, \delta_0)$ 

```

---

Algorithm 5 shows how a mix node processes a message it has received. First the message is unpacked into the header and the payload. Then the tag is derived and compared against previously seen  $tags$  to protect against replay attacks. Afterwards, the decryption verifies that the authentication tag matches the message and header metadata. Finally the header is unwrapped and a send operation is scheduled according to the next hop identifier and delay from the metadata.

---

**Algorithm 5** Processing of an incoming packet at mix node  $n$  with secret key  $x_n$ .

---

```

1: procedure  $PROCESS(packet)$ 
2:    $(M, \delta) \leftarrow packet$ 
3:    $s \leftarrow (M.\alpha)^{x_n}$ 
4:   if  $h_\tau(s) \in tags$  then abort
5:    $tags \leftarrow tags \cup \{h_\tau(s)\}$ 
6:    $\delta' \leftarrow AE_{dec}(s, \delta, M.\gamma, M.\beta)$ 
7:   if  $\delta' = \perp$  then abort
8:    $(n', delay), M' = PROCESSHEADER(M)$ 
9:    $QUEUEFORSEND(n', (M', \delta'), delay)$ 

```

---

## A.2 MultiSphinx (our solution)

We now describe our MultiSphinx construction and highlight the changes relative to the normal Sphinx construction in blue. To allow for a readable description we describe everything for  $p = 2$  however the general case follows easily.

We use the pseudo-random function (PRF)  $\rho$  together with its key-generating function  $h_\rho$  from the original Sphinx paper to create a deterministic pseudo-random padding. Since we need two derive to independent keys from the same secret,

we extend  $h_p$  with another parameter that can be an arbitrary string. This extension can be implemented using any suitable HKDF function.

Algorithm 6 explains the creation of MultiSphinx messages by the sender. The part concerning the “two legs” of the message graph is only shown once for A to allow for a more readable presentation. Line 21 instructs which lines are meant to be repeated for the other  $p - 1$  recipients. In line 4 the secret  $s_1$  is computed which is required for the padding construction in line 11. Lines 6-9 encrypt the actual payload from the recipient  $n_A$  to the multiplication node  $n_{1,A}$  (going backwards). The encrypted payloads  $\delta_{3,A}, \delta_{2,A}, \delta_{1,A}$  are all smaller than the normal payload length of messages. This would allow an attacker to distinguish such messages from other Loopix messages (e.g. when the middle mix layer sends loop messages). Therefore, the ciphertext is padded in line 11 with our PRF  $\rho$ . To correctly compute the MACs and headers in lines 15-20, we first simulate (going forwards) how the payloads will be affected by the decryption (line 12f).

Algorithm 7 explains the processing step at a mix node. Regular mix nodes operate as before (line 10). However, at multiplication nodes incoming message payloads are split into  $p$  headers and  $p$  payloads (line 12). In lines 13-16 the pseudo-random paddings are added. This process is also visualised in Figure 11. The newly created packets are processed recursively and then scheduled for sending based on their individual delay (line 15f). This “self-delivery” corresponds to the loop edge of  $n_1$  in Figure 10. The extra hop allows for delaying both messages independently at the multiplication node (two headers allow for two delays). It also simplifies our correctness arguments.

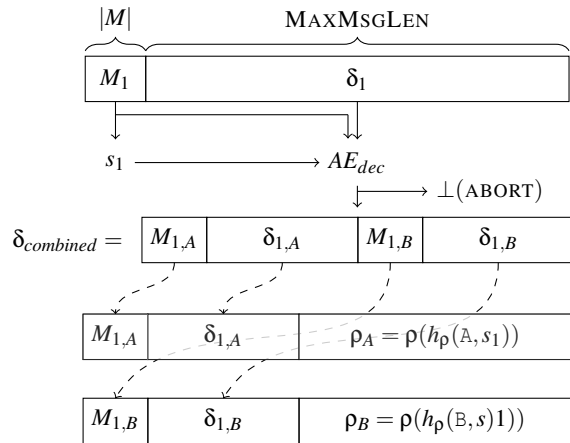


Figure 11: Processing of a MultiSphinx message at the multiplication node  $n_1$  resulting in two outgoing messages that are send then re-queued for processing.

**Algorithm 6** Creating a MultiSphinx packet to be routed through hops  $n_0, n_1, n_{2,A}, n_{2,B}$  to nodes  $n_A, n_B$ .

```

1: procedure CREATE( $\delta_A, \delta_B, n_0, n_1, n_{2,A}, n_{2,B}, n_A, n_B$ )
2:   assert  $|\delta_A| = |\delta_B| = (\text{MAXMSGLEN} - \text{HDRLEN})/2$ 
3:    $\triangleright$  Secrets for hops from sender to multiplier node  $n_1$ 
4:    $s_0, s_1 \leftarrow \text{COMPUTESECRETS}(n_0, n_1)$ 
5:    $\triangleright$  Encrypt from recipient  $n_A$  to multiplier node  $n_1$ 
6:    $s_{1,A}, s_{2,A}, s_A \leftarrow \text{COMPUTESECRETS}(n_{1,A}, n_{2,A}, n_A)$ 
7:    $\delta_{3,A} \leftarrow C(\text{KDF}(s_A, \text{cipher})) \oplus \delta_A$ 
8:    $\delta_{2,A} \leftarrow C(\text{KDF}(s_{2,A}, \text{cipher})) \oplus \delta_{3,A}$ 
9:    $\delta_{1,A} \leftarrow C(\text{KDF}(s_{1,A}, \text{cipher})) \oplus \delta_{2,A}$ 
10:   $\triangleright$  Add pseudo-random padding and compute padded
    payloads  $\delta'_{\dots}$  along decryption path
11:   $\delta'_{1,A} \leftarrow \delta_{1,A} \parallel \rho(h_p(A, s_1))$ 
12:   $\delta'_{2,A} \leftarrow C_{dec}(\text{KDF}(s_{1,A}, \text{cipher})) \oplus \delta'_{1,A}$ 
13:   $\delta'_{3,A} \leftarrow C_{dec}(\text{KDF}(s_{2,A}, \text{cipher})) \oplus \delta'_{2,A}$ 
14:   $\triangleright$  Compute headers and full MACs
15:   $M_{3,A} \leftarrow \text{CREATEHEADER}(s_A, *)$ 
16:   $M_{3,A}.\gamma \leftarrow \text{MAC}(\text{KDF}(s_A, \text{mac}), \delta'_{3,A} \parallel M_{3,A}).\beta$ 
17:   $M_{2,A} \leftarrow \text{CREATEHEADER}(s_A, n_{3,A}, M_{3,A})$ 
18:   $M_{2,A}.\gamma \leftarrow \text{MAC}(\text{KDF}(s_{2,A}, \text{mac}), \delta'_{2,A} \parallel M_{2,A}).\beta$ 
19:   $M_{1,A} \leftarrow \text{CREATEHEADER}(s_A, n_{2,A}, M_{2,A})$ 
20:   $M_{1,A}.\gamma \leftarrow \text{MAC}(\text{KDF}(s_{1,A}, \text{mac}), \delta'_{1,A} \parallel M_{1,A}).\beta$ 
21:  Repeat lines 6 – 20 for B
22:   $\triangleright$  From sender to multiplication node
23:   $\delta_{combined} = M_{1,A} \parallel \delta_{1,A} \parallel M_{1,B} \parallel \delta_{1,B}$ 
24:   $M_1 \leftarrow \text{CREATEHEADER}(s_1)$ 
25:   $\delta_1, M_1.\gamma \leftarrow \text{AE}_{enc}(s_1, \delta_{combined}, M_1.\text{METADATA})$ 
26:   $M_0 \leftarrow \text{CREATEHEADER}(s_0, n_1, M_1)$ 
27:   $\delta_0, M_0.\gamma \leftarrow \text{AE}_{enc}(s_0, \delta, M_0.\text{METADATA})$ 
28:  return  $(M_0, \delta_0)$ 

```

**Algorithm 7** Processing of an incoming packet at mix node  $n$  at mix layer  $l$  with secret key  $x^n$ .

```

1: procedure PROCESS( $packet$ )
2:    $(M, \delta) \leftarrow packet$ 
3:    $s \leftarrow (M.\alpha)^{x^n}$ 
4:   if  $h_\tau(s) \in tags$  then abort
5:    $tags \leftarrow tags \cup \{h_\tau(s)\}$ 
6:    $\delta' \leftarrow \text{AE}_{dec}(s, \delta, M.\gamma, M.\beta)$ 
7:   if  $\delta' = \perp$  then abort
8:    $n', delay, M' = \text{PROCESSHEADER}(M)$ 
9:   if  $l \neq 1$  then
10:     $\text{QUEUEFORSEND}(n', (M', \delta'), delay)$ 
11:  else
12:     $M_{1,A}, \delta_{1,A}, M_{1,B}, \delta_{1,B} \leftarrow \delta'$   $\triangleright \delta' = \delta_{combined}$ 
13:     $\rho_A, \rho_B \leftarrow \rho(h_p(A, s)), \rho(h_p(B, s))$   $\triangleright s = s_1$ 
14:     $\triangleright$  Process separately to allow independent delays
15:     $\text{PROCESS}(M_{1,A} \parallel \delta_{1,A} \parallel \rho_A)$ 
16:     $\text{PROCESS}(M_{1,B} \parallel \delta_{1,B} \parallel \rho_B)$ 

```

## B Algorithms

**Algorithm 8** The fault-tolerant Rollercoaster callback handler and send methods (signatures are checked implicitly).

---

```
1: procedure SENDTOGROUP(groupid, payload)
2:    $S \leftarrow \text{GENSCHEDULE}(msg.source, msg.groupid)$ 
3:   for recipient  $\in$  {direct children of self in  $S$ } do
4:      $msg \leftarrow \text{NEWMESSAGE}()$ 
5:      $msg.groupid \leftarrow groupid$ 
6:      $msg.nonce \leftarrow \text{FRESHNONCE}()$ 
7:      $msg.\{source, sender, role\} \leftarrow \text{self}$ 
8:      $msg.payload \leftarrow payload$ 
9:      $\text{SCHEDULEFORSEND}(recipient, msg)$ 
10:
11: procedure ONPAYLOAD(msg)
12:    $\text{APPLICATIONHANDLE}(msg.payload)$ 
13:   if msg was received while offline then return
14:   if msg was not seen before then
15:      $S \leftarrow \text{GENSCHEDULE}(msg.source, msg.groupid)$ 
16:     for  $x \in$  {direct children of msg.role in  $S$ } do
17:        $msg' \leftarrow \text{COPYMESSAGE}(msg)$ 
18:        $msg'.sender \leftarrow \text{self}$ 
19:        $msg'.role \leftarrow x$ 
20:        $\text{SCHEDULEFORSEND}(x, msg')$ 
21:    $\text{SCHEDULEFORSEND}(msg.source, \text{GENACK}(msg))$ 
22:
23: procedure ONACK(msg)
24:   assert ( $msg.source = \text{self}$ )
25:    $\text{CANCELTIMEOUT}(msg, msg.role, msg.sender)$ 
26:
27:    $\triangleright$  Called when a message leaves the payload queue
28: procedure ONMESSAGEISSENT(msg)
29:    $S \leftarrow \text{GENSCHEDULE}(msg.source, msg.groupid)$ 
30:   for  $x \in$  {recursive children of msg.role in  $S$ } do
31:      $timeout \leftarrow \text{ESTIMATETIMEOUT}(S, x)$ 
32:      $\text{ADDTIMEOUT}(msg, x, timeout)$ 
33:
34: procedure ONTIMEOUT(msg, recipientfailed)
35:    $S \leftarrow \text{GENSCHEDULE}(msg.source, msg.groupid)$ 
36:   if not  $\text{ISFORWARDINGNODE}(S, msg.role)$  then
37:     return
38:   for  $x \in$  {recursive children of msg.role in  $S$ } do
39:      $\text{CANCELTIMEOUT}(msg, msg.role, msg.sender)$ 
40:      $\triangleright$  timeout will be recreated when re-try is sent
41:      $recipient' \leftarrow \text{NEXTRECIPIENT}(S, recipient_{failed})$ 
42:      $\text{SCHEDULEFORSEND}(recipient', msg)$ 
43:      $msg.role \leftarrow \emptyset$   $\triangleright$  Re-try to failed node w/o role
44:      $\text{SCHEDULEWITHEXPBACKOFF}(recipient_{failed}, msg)$ 
```

---

**Algorithm 9** Methods explaining how the timeout information is stored and updated.

---

```
1: procedure ONINIT
2:    $\text{self.sessions} = []$   $\triangleright$  missing keys default to {}
3:
4: procedure ADDTIMEOUT(msg, role, recipient, timeout)
5:    $\text{CANCELTIMEOUT}(msg, role, recipient)$ 
6:    $id \leftarrow (msg.groupid, msg.nonce)$ 
7:    $entry \leftarrow (role, recipient, timeout)$ 
8:    $\text{self.sessions}[id] \leftarrow \text{self.sessions}[id] \cup \{entry\}$ 
9:
10: procedure CANCELTIMEOUT(msg, role, recipient)
11:    $id \leftarrow (msg.groupid, msg.nonce)$ 
12:    $session = \text{self.sessions}[id]$ 
13:    $\text{self.sessions}[id] \leftarrow \{x \in \text{self.sessions}[id] \mid x.role \neq role \wedge x.recipient \neq recipient\}$ 
```

---

**Algorithm 10** Determines whether node *node* is a forwarding node with regards to schedule  $S$ .

---

```
1: procedure ISFORWARDINGNODE( $S$ , node)
2:    $source \leftarrow S[0][0][0]$ 
3:   if  $node = source$  then
4:     return false
5:   for  $t = 1$  until  $|S|$  do
6:      $R \leftarrow S[t]$ 
7:     for (sender,  $\_$ ) in  $R$  do
8:       if  $node \neq source$  and  $node = sender$  then
9:         return true
10:   return false
```

---

## C Extended Paper

The extended paper is available at: <https://www.cl.cam.ac.uk/techreports/UCAM-CL-TR-957.html>. Its additional appendices contain: a proof for eventual delivery of Rollercoaster, a security proof for MultiSphinx, visualisations of the offline models, histogram plots of latency distributions, and additional heatmap figures. The main text of the extended paper only differs from this paper where it references these additional pieces of information.